# *Essential roles of fibronectin in the development of the left–right embryonic body plan*



**Citation:** Pulina, Maria V., Shuan-Yu Hou, Ashok Mittal, Dorthe Julich, Charlie A. Whittaker, Scott A. Holley, Richard O. Hynes, and Sophie Astrof. "Essential roles of fibronectin in the development of the left–right embryonic body plan." Developmental Biology 354, no. 2 (June 2011): 208-220.


**As Published:** http://dx.doi.org/10.1016/j.ydbio.2011.03.026

**Publisher:** Elsevier

**Persistent URL:** http://hdl.handle.net/1721.1/84535

**Version:** Final published version: final published article, as it appeared in a journal, conference proceedings, or other formally published context

Developmental Biology 354 (2011) 208–220

Contents lists available at ScienceDirect

Developmental Biology

journal homepage: www.elsevier.com/developmentalbiology

# Essential roles of fibronectin in the development of the left–right embryonic body plan

Maria V. Pulina [a,1], Shuan-Yu Hou [a,2], Ashok Mittal [a,3], Dorthe Julich [b], Charlie A. Whittaker [c], Scott A. Holley [b], Richard O. Hynes [c,d], Sophie Astrof [a,*,2]

[a] Weill Cornell Medical College, Department of Medicine, Division of Cardiology, New York, NY, USA
[b] Department of Molecular, Cellular and Developmental Biology, Yale University, New Haven, CT, USA
[c] David H. Koch Institute for Integrative Cancer Research, Massachusetts Institute of Technology, Cambridge, MA, USA
[d] Howard Hughes Medical Institute, Chevy Chase, Maryland, USA

ARTICLE INFO

*Article history:*
Received for publication 3 December 2010
Revised 14 March 2011
Accepted 28 March 2011
Available online 3 April 2011

*Keywords:*
Fibronectin
Integrin alpha 5
Left–right asymmetry
Nodal
Lefty
Pitx2c
SMAD

ABSTRACT

Studies in *Xenopus laevis* suggested that cell-extracellular matrix (ECM) interactions regulate the development of the left–right axis of asymmetry; however, the identities of ECM components and their receptors important for this process have remained unknown. We discovered that FN is required for the establishment of the asymmetric gene expression pattern in early mouse embryos by regulating morphogenesis of the node, while cellular fates of the nodal cells, canonical Wnt and Shh signaling within the node were not perturbed by the absence of FN. FN is also required for the expression of *Lefty 1/2* and activation of SMADs 2 and 3 at the floor plate, while cell fate specification of the notochord and the floor plate, as well as signaling within and between these two embryonic organizing centers remained intact in FN-null mutants. Furthermore, our experiments indicate that a major cell surface receptor for FN, integrin $\alpha5\beta1$, is also required for the development of the left–right asymmetry, and that this requirement is evolutionarily conserved in fish and mice. Taken together, our studies demonstrate the requisite role for a structural ECM protein and its integrin receptor in the development of the left–right axis of asymmetry in vertebrates.



## Introduction

Left–right (L–R) axis determination occurs early during embryonic development and is critical for establishing the correct body plan in vertebrates since a number of visceral organs are asymmetrically located within the body. Asymmetric development of a number of organs is requisite for their normal function, for instance, the incidence of congenital heart disease increases from 0.1% observed in general population to 3–90% in humans with L–R disorders (Ramsdell, 2005).

In the mouse, the breaking of the symmetrical embryonic body plan results from the leftward flow generated inside a pit-like structure on the ventral side of the embryo, called the node, which forms around embryonic (E) day 7.5 of mouse development. The leftward flow is generated by the clockwise (if viewed ventrally) rotation of monocillia protruding from each cell of the node, facilitating asymmetrical expression of *Nodal* mRNA at the left rim of the node, which is essential for the establishment of the asymmetrical gene expression pattern and subsequent asymmetrical organ development (Brennan et al., 2002; Nonaka et al., 2002; Oki et al., 2009).

The node arises from cells at the anterior end of the primitive streak (PS) (Kinder et al., 2001). Cells of the future node, initially located underneath the visceral endoderm, move ventrally and intercalate between the cells of the visceral endoderm, becoming visible on the embryonic surface as a single field of tiny ciliated cells by E7.5 (Lee and Anderson, 2008; Lee et al., 2010; Sulik et al., 1994). By about E7.75, the node appears as an indentation of about 50 μm deep and is composed of two layers of cells. The ventral-most cell layer is made of cells with small apical surfaces and a single cilium protruding from the posterior end of each cell at an acute angle (Lee and Anderson, 2008; Sulik et al., 1994). Mutations that disrupt formation of the normal shape of the node, or a functionally similar structure in teleost fish, called the Kupffer's vesicle, lead to defects in asymmetric gene expression and disrupt the canonical L–R morphogenesis (Amack et al., 2007; Lee and Anderson, 2008; Lee et al., 2010). The node is thus the key early embryonic structure required for the establishment of L–R asymmetry in the mouse (Lee and Anderson, 2008; Shiratori and Hamada, 2006).

* Corresponding author at: Jefferson Medical College, 1025 Walnut Street; Suite 314, Philadelphia, PA 19107, USA. Fax: +1 215 955-9992.
*E-mail address:* sophie.astrof@gmail.com (S. Astrof).
[1] Current address: Program in Developmental Biology, Memorial Sloan-Kettering Cancer Center, New York, NY, USA.
[2] Current address: Jefferson Medical College, Thomas Jefferson University, Department of Medicine, Center for Translational Medicine, Philadelphia, PA, USA.
[3] Current address: Jacobi Medical Center of Albert Einstein College of Medicine, Department of Medicine, Bronx, NY, USA.

0012-1606/$ – see front matter © 2011 Elsevier Inc. All rights reserved.
doi:10.1016/j.ydbio.2011.03.026

Seminal studies conducted in the 1990s, suggested that the surface ectoderm of the early *Xenopus laevis* gastrula carries essential information for directing orientation of asymmetrically developing organs along the L–R axis (Yost, 1992). The surface ectoderm facing the blastocoel roof in these early embryos assembles fibronectin (FN) fibrils, and injection of the Arg-Gly-Asp (RGD) but not the Arg-Gly-Glu (RGE) peptides into the blastocoel cavity led to randomization of L–R orientation of the heart and the gut with concomitant disruption of FN matrix assembly on the ectodermal surface. Presumably, these defects were due to the competition of the exogenously added RGD peptides with cell surface integrins for the binding to the RGD motif of FN and/or to RGD motifs within other ECM components, potentially disrupting cell-ECM interactions. Additional experiments in *Xenopus* and in cell culture showed that cell-surface syndecan-2 mediates FN fibrillogenesis and cell spreading, and is required for L–R asymmetric development (Klass et al., 2000; Kramer and Yost, 2002; Saoncella et al., 1999). Recent studies also showed that integrin subunits αv and β1d are required for the morphogenesis of the Kupffer's vesicle and the establishment of L–R asymmetry in fish (Ablooglu et al., 2010). Taken together, these studies suggest that interactions of cells with the ECM (and possibly with FN) are important for the development of the asymmetric body plan in vertebrates. However, the role of the ECM in L–R development, the identity of ECM component(s), their cellular receptors, as well as the morphogenetic and molecular processes they regulate during the development of L–R axis have remained largely unknown.

FN is an essential component of the extracellular matrix, as mice lacking FN die between E9.5 and E10.5 with defects that vary in severity depending on their genetic background (Astrof et al., 2007b; George et al., 1997). Functions of FN have been analyzed in zebrafish, frogs and mice using a range of approaches including mutagenesis, morpholinos and function blocking antibodies (Davidson et al., 2002, 2006; George et al., 1997, 1993; Georges-Labouesse et al., 1996; Marsden and DeSimone, 2001, 2003; Trinh and Stainier, 2004). The main conclusions that have emerged from these analyses can be summarized as follows: 1) major movements of gastrulation giving rise to the three germ layers, the ectoderm, mesoderm and endoderm, proceed in the absence of FN (Davidson et al., 2002; George et al., 1993; Georges-Labouesse et al., 1996; Marsden and DeSimone, 2003; Trinh and Stainier, 2004); 2) specification of cell fates including axial, paraxial and lateral mesoderm, differentiation of mesodermal precursors into somitic or cardiomyocitic lineages takes place in the absence of FN (George et al., 1997; Georges-Labouesse et al., 1996; Trinh and Stainier, 2004); 3) the relative positions of lineages and precursors are comparable between embryos lacking or containing FN protein (Davidson et al., 2006; George et al., 1997; Georges-Labouesse et al., 1996; Trinh and Stainier, 2004); and 4) specification and migration of lineages that arise following gastrulation, such as the neural crest, do not depend on FN (Mittal et al., 2010). Despite grossly normal cell fate specification, as well as differentiation and migration of diverse embryonic lineages, FN mutant fish, mouse and frog embryos, in which FN protein was depleted using various methods, show severe defects in the overall embryonic morphogenesis, and in particular, the formation of somites from somite precursors, the heart from cardiac precursors and the morphogenesis, of the notochordal plate into a chord (Davidson et al., 2002, 2006; George et al., 1997; Georges-Labouesse et al., 1996; Marsden and DeSimone, 2001; Trinh and Stainier, 2004). Investigations into the underlying causes of these morphogenetic defects in fish and frog pointed to an integral role of FN in regulating cell shape, cell-cell adhesion (activation of cadherins) and cell polarity, as well as in regulating frequency, stability and directionality of cellular protrusions (such as lamellipodia), directed cellular movements, orchestrating convergence and extension, epiboly, and the coalescence of the bilateral cardiac primordia into a single heart tube (Davidson et al., 2002, 2006; Marsden and DeSimone, 2001; Trinh and Stainier, 2004). Interestingly, experiments with frog tissue explants and frog embryos treated with antibodies blocking cell binding to FN, demonstrated that cell adhesion to FN is required for the thinning of the blastocoel roof by regulating vertical intercalation of cells situated some distance away from the substratum, suggesting that cell polarizing activity of FN can be propagated across cell layers (Marsden and DeSimone, 2001). These experiments and others also pointed to an important role of α5β1 integrin in mediating cellular responses to FN (Davidson et al., 2002, 2006; Julich et al., 2005, 2009; Marsden and DeSimone, 2001; Takahashi et al., 2007). However, the role of FN in orchestrating mammalian development is not well understood.

In the studies presented below, we tested the hypothesis that FN and one of its major cellular receptors, integrin α5β1, orchestrate the development of L–R body axis in the mouse. Our data indicate that during early mouse embryogenesis, FN plays an essential role in the development of the L–R asymmetry. Initially and primarily, it is essential for the morphogenesis of the node. In the absence of FN, the node appears disrupted, narrow and flat, and is composed of multiple layers of aberrantly oriented cells, instead of two well-organized cell layers. In a separate set of experiments, we analyzed cell fate specification of the floor plate and the notochordal plate. We found that a fairly contiguous, albeit thin, notochordal plate forms in early FN mutants and that FN was not required for cell fate specification of the notochordal plate or the floor plate, or for the communication between these important signaling centers. However, in contrast to control embryos, *Lefty1 and 2* mRNAs were not expressed in the floor plate of FN-nulls and we found a lack of enrichment in phosphorylated, activated forms of SMADs 2 and 3 in the floor plate of FN mutants. These observations point to a potential second role of FN, namely, in the establishment and/or maintenance of the midline barrier function. Finally, we demonstrate that one of the major cellular receptors for FN, integrin α5β1, is also required for the development of L–R asymmetry and that this requirement is conserved in mice and fish. Taken together, our experiments point to a novel role of the ECM during the development of the L–R axis of asymmetry.

## Materials and methods

### *Embryo collection*

All mouse strains were of 129S4 genetic background. FN-null mouse embryos were obtained by mating FN-heterozygous (het) males and females (George et al., 1993). Integrin α5-null embryos were obtained from crossing integrin α5-het mice (Yang et al., 1993). The day when the plugs were found was considered E0.5. Embryos were collected in the early morning of E8.5, providing mutants (which lack somites) and control littermates containing 0–6 somites. Zero-somite embryos corresponded with the late headfold (LHF) stage of development (Downs and Davies, 1993). Yolk sacs were genotyped by PCR, as described (George et al., 1993; Yang et al., 1993). Maternal-zygotic integrin α5-null embryos were collected from crossing integrin α5-null adult zebrafish mutants, generated as described (Julich et al., 2005).

### *Microarray analysis*

Three FN-null embryos from 129S4 strain and four FN-null embryos from C57BL6/J strain were used. Wild-type embryos (four from each genetic background) containing 6 somites were used as controls. mRNA was extracted from each embryo, amplified and labeled, as described (Astrof et al., 2007b). mRNAs from each embryonic sample were analyzed as separate biological and experimental replicates. Gene expression was assayed using Affymetrix 430 2.0 arrays, as described (Astrof et al., 2007b).

*Whole mount in situ hybridization*

Embryos were collected in ice cold phosphate buffered saline (PBS) and fixed in 4% buffered paraformaldehyde (PFA) for 24 h at 4 °C. Embryos were then washed twice in PTW (PBS/0.1%Tween-20), dehydrated in graded series of methanol and stored in 100% methanol at −20 °C. Whole mount *in situ* hybridization was performed, as described http://www.sickkids.ca/research/rossant/protocols/Conlon/WM2_Henrique.pdf (Henrique et al., 1995). The following plasmids were obtained for *in vitro* transcription of anti-sense riboprobes: *Nodal* (from Dr. Daniel Constam), *Lefty1/2* (from Dr. Hiroshi Hamada), *Pitx2c* (from Dr. James Martin), *Shh* and *Ptch1* (originally from Dr. Andrew McMahon), *Brachyury* (originally from Dr. Rosa Beddington), *FoxA2* and *Bmp4* (from Dr. Brigit Hogan). Stained embryos were photographed using Zeiss Stemi 2000-C microscope and Leica DFC 420 camera. The node width was determined by measuring the distance between the stripes of *Nodal* mRNA at either side of the node using Image J. The width was measured at the widest part of the node three times per embryo and the measurements were averaged for each embryo. Control and mutant embryos were kept together in one tube at all stages of staining, development and photography to avoid variability due to handling.

*Scanning electron microscopy*

Embryos were dissected either at E7.75 or on the morning of E8.5. This allowed us to collect embryos ranging from E7.5 to E8.5 in development, corresponding with the late bud (LB) to the LHF stages described in (Downs and Davies, 1993). Embryos were fixed in 0.25% glutaraldehyde in PBS for at least 48 h at 4 °C, dehydrated in graded series of ethanol and stored in 100% ethanol at −20 °C until use. Embryos were critical-point dried and mounted using a sewing needle onto a double-sided adhesive tape attached to a metal stub. Embryos were then coated with gold/palladium in a DentonVacuum Desk IV sputter coater and photographed using Zeiss Field Emission Scanning Electron Microscope Supra 25.

*Whole mount immunofluorescence and confocal microscopy*

Embryos were dissected in the morning of E8.5. At this time, control embryos ranged between 0 somites, corresponding with the LHF stage of development, and 6 somites. Embryos were fixed in 4% PFA at 4 °C overnight (O/N), washed in PBS several times and stored at 4 °C for no more than 2 weeks. Embryos were blocked in 10% donkey serum in PBS/0.1% Triton X-100 (PBST) at 4 °C O/N. The following primary antibodies were used: rabbit polyclonal anti-FN antibody, clone 297.1 (George et al., 1997) at 1:500 dilution, rabbit polyclonal anti-FoxA2 antibody (Abcam, cat # ab40874) at 1:100 dilution. 1 mg/ml DAPI (Sigma-Aldrich) was diluted 1:1000 and used to stain nuclei for 1 h at room temp. After the incubation with primary antibodies O/N at 4 °C, embryos were extensively washed in 10% donkey serum/PBST, and incubated with Alexa-488-labeled secondary antibodies (Molecular Probes) in blocking solution O/N and washed again in 10% donkey serum/PBST. Embryos were mounted onto glass slides using Prolong Gold antifade reagent (Molecular Probes) and coverslipped. Images were taken using inverted LSM510 laser scanning confocal microscope (Zeiss). Z stacks were taken at 0.4–0.5 μm intervals through the thickness of the entire embryo. 3D reconstructions of zstacks were done using Imaris (Fig. 2C or Movie 1) or Zeiss LSM software.

*Whole mount immunostaining*

Embryos were dissected at E8.5, as above. Following fixation in 4% PFA at 4 °C O/N, embryos were washed in PBS several times and stored at 4 °C for no more than 2 weeks. Embryos were blocked in 10% donkey serum in PBS/0.05% Tween-20 at 4 °C O/N and subsequently incubated with anti-FN primary rabbit polyclonal antibody at 1:500 dilution O/N in blocking solution, or with rat monoclonal anti-Itga5 antibody at 1:75 dilution (Pharmingen cat# 553319). Embryos were extensively washed in blocking solution and incubated with Biotin-SP conjugated anti-rabbit (or anti-rat) secondary antibodies (Jackson Immunoresearch Laboratories, Inc) in blocking solution O/N. After several washes, staining was developed using the DAB kit (Vector Laboratories, Inc). Control stainings were performed using normal rabbit or rat IgG and resulted in minimal background. To detect activated forms of SMADs 2/3, embryos were fixed in 4% PFA for 2 h at room temperature, washed 2 times in PBT (PBS/0.5% Tween-20), dehydrated in graded series of MeOH/PBT and stored in methanol at −20 °C until use. Before staining, embryos were rehydrated to PBT, incubated with $H_2O_2$ for 1 h in PBS and then blocked in 10% donkey serum in PBT. Embryos were then incubated with the rabbit polyclonal antibodies raised to recognize phosphorylated serines 465 and 467 of SMAD 2 and reactive with active forms of both SMADs 2 and 3 (Cell Signaling Technology, cat # 3101). Antibodies were diluted in 10% donkey serum /PBT and incubations were carried out at 4 °C O/N. Embryos were then extensively washed in blocking solution and incubated with HRP-conjugated secondary antibody O/N at 4 °C in blocking solution. Staining was developed using the DAB kit. Control and mutant embryos were kept together at all times during staining, color development and photography to avoid differences due to handling. These experiments were performed at least four independent times.

## Results

*Fibronectin is required for the development of the left–right embryonic body axis*

In the course of our studies to identify the genetic modifier(s) modulating the severity of cardiac defects in FN-null embryos isolated from 129S4 and C57BL6/J strains of mice, we performed a microarray analysis and found that independent of the genetic background, *Nodal* and *FoxH1* mRNAs were downregulated in FN-null embryos (n = 7) compared with wild-type controls isolated at E8.5 and containing 6 somites (n = 8). *Nodal* mRNA was downregulated 4.9-fold (adjusted p = 0.02) and *FoxH1* mRNA was downregulated 2.4-fold (adjusted p = 0.007) in FN-null embryos compared with controls. Given the integral role of *Nodal* and *FoxH1* in the establishment of L–R axis of asymmetry, and the studies performed in the early 1990s showing randomization of L–R asymmetry in frog embryos injected with RGD peptides (Yost, 1992), the ostensible deregulation of *Nodal* and *FoxH1* expression in FN-null mouse mutants suggested that FN could be important for the development of the L–R body plan.

Expression levels and the spatial distribution of *Nodal* mRNA are dynamically regulated and vary widely during the course of early vertebrate embryogenesis (Levin et al., 1995; Shiratori and Hamada, 2006). Since FN-null embryos do not develop somites (George et al., 1993; Georges-Labouesse et al., 1996), it is challenging to precisely determine the developmental stage of FN-null embryos, which could have resulted in the potential deregulation of *Nodal* levels between the wild-type and FN-null embryos assayed by microarray analysis. Since distinctive asymmetric expression of *Nodal* around the midline is a general requirement for L–R axis development in all of the Bilateria (Grande and Patel, 2009), we performed *in situ* hybridization (ISH) experiments using FN-null and control embryos to visualize spatial expression patterns of *Nodal* and other genes, such as *Lefty1*, *Lefty2* and *Pitx2c* known to be asymmetrically expressed (Lee and Anderson, 2008). During the normal course of embryogenesis, *Nodal* mRNA is expressed on both sides of the node. Initially, this expression is symmetrical, but by about 2-somite stage, the expression of *Nodal* mRNA becomes enriched at the left rim of the node and the left side of the lateral plate mesoderm (LPM) (Yamamoto et al., 2001). We found that the expression of *Nodal* mRNA around the node was disturbed in

FN-null embryos (Figs. 1A–E). While in controls we observed either symmetrical stripes of *Nodal* mRNA (8/11 embryos) at the left and right sides of the node, or an enrichment of *Nodal* mRNA at the left rim of the node (in 3/11 embryos), the expression of *Nodal* mRNA around the node in FN-nulls was disorganized (Table 1). In 5/11 mutants, *Nodal* mRNA was clearly enriched at the right rim of the node (Figs. 1C and D). In the remainder of FN-nulls, the pattern of *Nodal* mRNA at the node seemed normal: in 5/11 FN-nulls *Nodal* mRNA was symmetrically expressed around the node and in 1/11 mutants *Nodal* mRNA was enriched at the left rim. However, the two stripes of *Nodal* mRNA around the node were often distorted in shape (e.g. Supplemental Fig. 1B). In 2/11 FN-null embryos, the stripes of *Nodal* mRNA demarcating the node appeared to be located toward the left (1/11) or the right (1/11) side of the embryonic midline (Fig. 1D and Sup. Fig. 1B). We also observed asymmetric position of the node relative to the embryonic midline by scanning electron microscopy (SEM) in three out of 13 examined FN-null embryos (Sup. Fig. 1D).

The enrichment of *Nodal* mRNA on the left side of the node with respect to the right is essential for the establishment of the asymmetrical gene expression program around the midline during mammalian embryogenesis (Nakamura et al., 2006; Oki et al., 2009). Therefore, deregulation of *Nodal* mRNA expression around the node in FN-null embryos, suggested that asymmetric pattern of gene expression of *Nodal*, *Lefty2* and *Pitx2c* mRNAs in the left LPM may be disturbed as well. Indeed, our ISH experiments showed that the expected spatial pattern of *Nodal* mRNA expression in the LPM was deregulated in FN-nulls (Figs. 1A–E), Table 2. While in all controls (n = 6), *Nodal* mRNA was detected only at the left LPM, only in 3 out of 9 FN-null embryos *Nodal* mRNA was confined to the left side. In 2/9 mutants, *Nodal* was expressed on both sides of the LPM, in one embryo it was found only on the right side, and in 3/9 FN-null embryos, *Nodal* mRNA was absent from the LPM altogether. The variability in L–R gene expression observed in our mutants is characteristic of many published mutants with deregulated left–right body plan. This variability can be explained by computational models describing how left–right body plan is established (Nakamura et al., 2006).

**Table 1**
*Nodal* mRNA around the node.

| | L>R | L=R | L<R | R only |
|---|---|---|---|---|
| Control | 7 / 27 | 11 / 27 | 1 / 27 | 0 |
| FN-null | 1 / 11 | 5 / 11 | 5 / 11 | 0 |
| Integrin α5-null | 8 / 17 | 3 / 17 | 4 / 17 | 2 / 17 |

Pink shading represents the presence of hybridization signal. Note that the increased *Nodal* mRNA signal on the right side of the node is observed in nearly half of FN-null mutants, while only 1 out of 27 controls showed a slightly increased *Nodal* expression on the right side.

Similarly to *Nodal*, left-sided expression of *Lefty2* and *Pitx2c* in the LPM is a characteristic feature of normally developing L–R embryonic body plan in vertebrates (Lee and Anderson, 2008). While in control embryos the expression of *Lefty2* and *Pitx2c* mRNA was confined to the

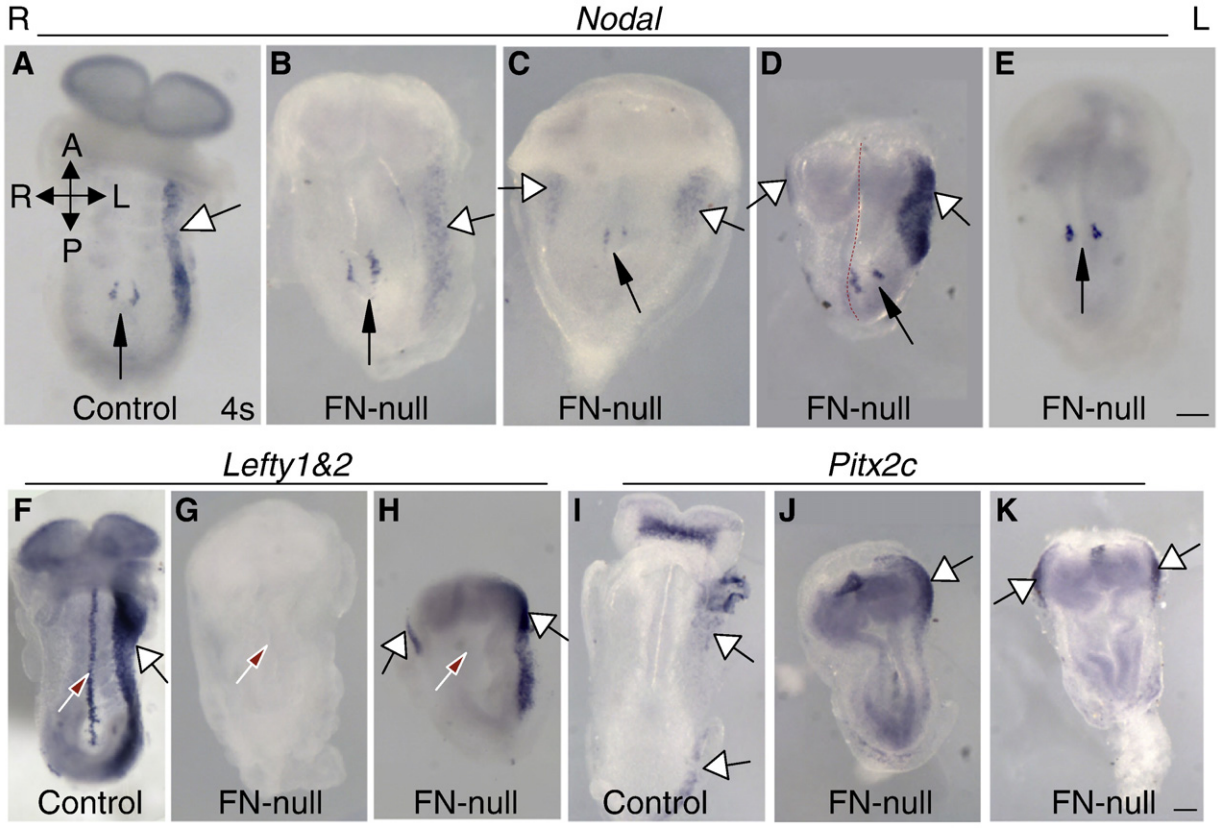


**Fig. 1.** FN is required for the asymmetric expression of *Nodal*, *Lefty* and *Pitx2c*. A–E. Expression of *Nodal* mRNA in control (A) and FN-null (B–E) embryos at approximately E8.25. B. A relatively normal expression of *Nodal* in the left LPM (white arrow) and around the node (black arrow). C. Expression of *Nodal* mRNA is enriched on the right side of the node and is present both in the right and left LPM. D. In this FN-null embryo, the node (black arrow) is positioned to the left of the embryonic midline (red dashed line) and the expression of *Nodal* mRNA is enriched on the right side of the node. Ectopic *Nodal* mRNA is present in the anterior right LPM. E. *Nodal* mRNA is absent in the LPM of this well-developed FN-null embryo. All pictures in A–E were taken at the same magnification. F–H. Expression of *Lefty1* and *Lefty2* mRNA in control (F) and FN-null embryos (G–H). Absent (G) and bilateral (H) expression of *Lefty2* in the LPM. Red arrow points at the midline in control and at the presumed midline in FN-nulls, white arrows point at the LPM. Note the absence of midline staining in FN-null embryos. I–K. Expression of *Pitx2c* mRNA in control (I) and FN-null embryos (J–K). Left-restricted (J) and bilateral (K) expression of *Pitx2c* in FN-null embryos. Ventral views are presented in all pictures, A—anterior, P—posterior, R—right and L—left axes are indicated at the top of the figure. All pictures in F–K were taken at the same magnification. Scale bars are 100 μm.

**Table 2**
*Nodal* mRNA in the LPM.

| | Left only | Right only | Lefty & Right | None |
|---|---|---|---|---|
| Control | 19 / 22 | 0 / 22 | 0 / 22 | 0 / 22 |
| FN-null | 3 / 9 | 1 / 9 | 2 / 9 | 3 / 9 |
| Integrin α5-null | 3 / 17 | 0 / 17 | 4 / 17 | 10 / 17 |

Pink shading represents the presence of hybridization signal.

**Table 4**
*Pitx2c* mRNA in the LPM.

| | Left only | Lefty & Right |
|---|---|---|
| Control | 8/8 | 0/8 |
| FN-null | 1/3 | 2/3 |
| Integrin α5-null | 1/2 | 1/2 |

Pink shading represents the presence of hybridization signal.

left LPM (3 controls were examined in each case), *Lefty2* mRNA was found on either the left (2/7 embryos), the right (1/7), or both sides (2/7) of the LPM in FN-null embryos or was not expressed in the LPM at all (2/7) (Figs. 1F–H), Table 3. The expression of *Pitx2c* in the LPM was also deregulated in FN-nulls (Figs. 1I–K). *Pitx2c* was localized to the left (1/3 embryos) or seen on both sides (2/3 embryos) in the mutants, Table 4. Notably, we did not detect the expression of *Lefty1* or *2* in the midline of 7 examined FN-null embryos (e.g. Figs. 1G and H).

It is important to note that the Nodal signaling axis is functional in the LPM of FN-null embryos analyzed. Evidence from prior genetic studies allowed a general inference that Nodal protein expressed at the node travels to the LPM where it signals through Nodal receptors, e.g. ActRIIB, co-receptor, EGF-CFC and transcription factor FoxH1 to induce the expression of itself, *Lefty1, 2* and *Pitx2c* (Bamford et al., 2000; Brennan et al., 2002; Marjoram and Wright, 2011; Nakamura et al., 2006; Norris et al., 2002; Oh and Li, 1997; Oki et al., 2009; Saijoh et al., 2000; Sakuma et al., 2002; Yan et al., 1999; Yoshioka et al., 1998). The expression of *Nodal*, *Lefty2* and *Pitx2c* mRNAs in the LPM of FN-null embryos suggests that the spread of Nodal from the node to the LPM as well as Nodal signaling to the LPM does not depend on FN (Fig. 1). Taken together with prior studies in fish, frogs and mice, which demonstrated spatially correct specification of various lineages in mutants lacking FN or depleted of FN protein (Davidson et al., 2002, 2006; George et al., 1997; Georges-Labouesse et al., 1996; Mittal et al., 2010; Trinh and Stainier, 2004), the spatially deregulated expression patterns of *Nodal*, *Lefty2* and *Pitx2c* mRNAs around the midline in FN-null embryos indicate a specific and requisite role of FN during the development of the L–R axis of asymmetry.

### *Fibronectin is enriched at the borders of the node, notochord and the floor plate*

In order to gain insights into the function of FN during the development of the L–R embryonic body plan, we analyzed expression of *FN* mRNA and protein during early mouse embryogenesis. *FN* mRNA is expressed bilaterally at 1-somite stage (Fig. 2A). When embryos develop 2 somites, *FN* mRNA becomes expressed in large cells on either side of the node, and observation of whole embryos (n = 6) suggested that *FN* mRNA is expressed fairly symmetrically around the node (Fig. 2B, B1 and data not shown). The large cells expressing *FN* mRNA around the node are most likely to be of visceral endodermal origin (Fig. 2B1) (Kwon et al., 2008).

**Table 3**
*Lefty2* mRNA in the LPM.

| | Left only | Right only | Lefty & Right | None |
|---|---|---|---|---|
| Control | 11 / 11 | 0 | 0 | 0 |
| FN-null | 2 / 7 | 1 / 7 | 2 / 7 | 2 / 7 |
| Integrin α5-null | 1 / 7 | 3 / 7 | 3 / 7 | 0 |

Pink shading represents the presence of hybridization signal.

FN protein is enriched at the borders of the node and the notochord (Fig. 2C–C2) and localizes at the basal surfaces of the notochordal plate and the ventral node (Fig. 2C3–4). Interestingly, similar to the enrichment of the *Nodal* mRNA at the left rim of the node in 2–3-somite wild-type embryos, we observed an elongated domain of FN protein expression on the left side of the node, compared with the right, in 5 out of 6 wild-type embryos with two or more somites by using either confocal immunofluorescence (IF) microscopy or immunohistochemistry (IHC) (Fig. 2C1–2, arrows, and data not shown). We speculate, that this enrichment of FN protein at the left side is due to a potential enrichment of FN-binding integrins at the left side of the node compared with the right side. This expression pattern of FN protein suggested that FN may play specific role(s) during node morphogenesis and the establishment of L–R asymmetry.

We reasoned that enrichment of FN at the borders of the node and the notochordal plate (Fig. 2C2 and Sup. Movie 1) could be due to the presence of FN-binding integrins. Integrins are heterodimers of different alpha and beta chains, with each chain encoded by a distinct gene. These cell surface proteins function as a major class of ECM receptors. There are twenty four known integrin heterodimers (Hynes, 2002), among which integrins α5β1, αvβ1, αvβ3, αvβ8, α4β1, α4β7, α3β1, and α8β1 bind FN *in vitro* and signal (van der Flier and Sonnenberg, 2001). Mouse embryos lacking integrin β1 subunit, a mutation eliminating 12 known integrin heterodimers, die at peri-implantation stages of development (Fassler and Meyer, 1995; Hynes, 2002; van der Flier and Sonnenberg, 2001). Individual deletion of integrin α chains listed above indicated that the phenotype of integrin α5 mutant mouse embryos is by far most severe, compared with individual deletion of any other integrin α subunit, and is the most similar to the phenotype FN-null mutants (Bader et al., 1998; Chan et al., 2010; Yang et al., 1999), suggesting that integrin α5β1 acts as the main, although not the only, FN receptor during early embryonic development. We found that similar to FN, integrin α5 is also enriched at the borders of the node, and to some degree at the borders of the notochordal plate (Fig. 7D). Analysis of tissue sections indicated that integrin α5 localizes to the basal side of the ventral node and notochordal plate (Fig. 7D1 and data not shown), the surfaces enriched in FN protein (Fig. 2C3–4), suggesting that integrin α5β1 could facilitate assembly of FN fibrils at these borders. Indeed, we observed that the absence of integrin α5 leads to defective pattern of distribution of FN protein around the node and in the LPM (Sup. Fig. 4). This pattern is suggestive of defective assembly of FN into higher order fibrils (Davidson et al., 2008; Ohashi et al., 1999). However, enrichment of FN around the notochordal plate remained grossly intact in integrin α5-null mutants (Sup. Fig. 4), suggesting that other (or multiple) FN-binding integrins may be involved in localizing FN protein to the notochordal borders.

### *FN is required for the morphogenesis of the node*

Since our expression studies indicated that *FN* mRNA and protein were enriched at the node (Figs. 2B and C), we reasoned that FN could be important for the morphogenesis and/or function of this structure. Formation of the node, nodal cilia, and signaling by growth factors

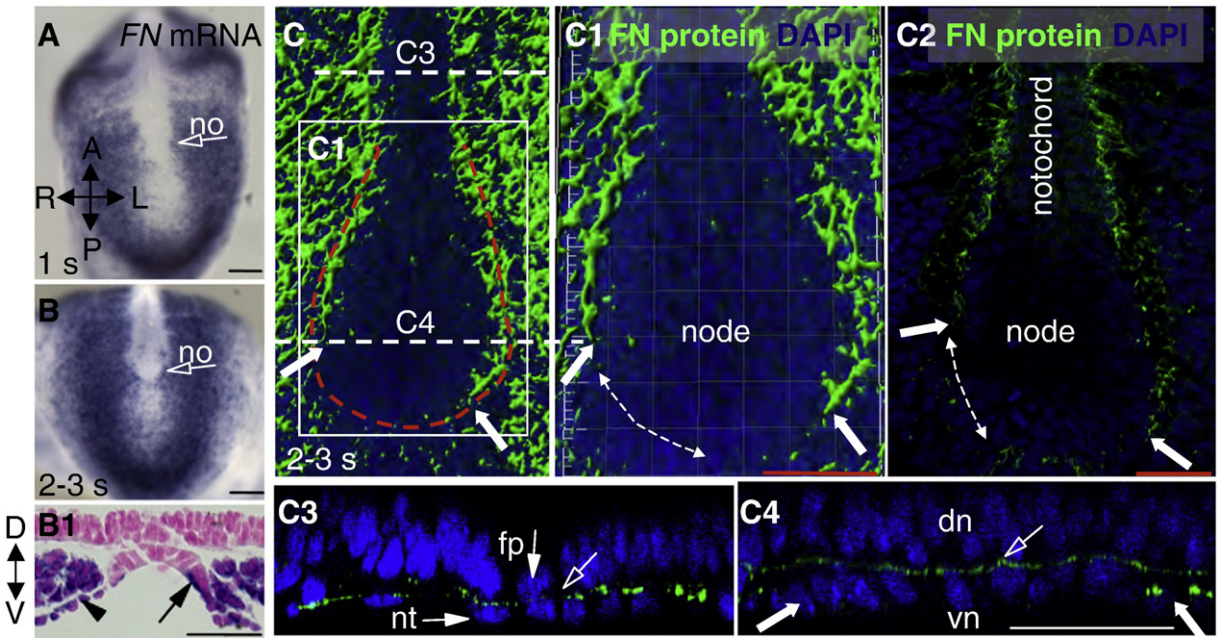


**Fig. 2.** Expression of *FN* mRNA and protein in developing embryos. A–B1. *FN* mRNA staining. A. *FN* mRNA is expressed in the LPM in a one somite (s) embryo. Note undetectable levels of *FN* mRNA in the embryonic midline in A–B. B. Expression of *FN* mRNA by cells around the node (no, arrow). Transverse section at the level of the node (arrow) is shown in B1. Note expression of *FN* mRNA by the presumptive crown cells (arrow) and endoderm (arrowhead). The section is skewed toward one side creating impression of asymmetric *FN* mRNA distribution. C. FN protein staining. 3D reconstruction of confocal sections through the embryo. FN staining in 2–3 somite (s) control embryo shows the domain of FN protein (green) is extended posteriorly at the left side of the node (red dotted line). Boxed area is expanded in panel C1. Filled arrows point to the extent of FN staining on the left and right sides of the node. Dashed lines indicate orthogonal confocal slices shown in C3 and C4. C1. Expanded view of the node 3D reconstruction. C2. An optical z slice in xy plane, close to the center of the embryo (in the dorsal-to-ventral direction). Dashed double-headed arrows outline the region of the node on the right devoid of FN (C1–C2). C3. Orthogonal view through the notochord. FN (open arrow) is localized between the notochordal plate and the floor plate (fp). C4. Orthogonal view through the node shows that FN protein localizes to the basal surface of the ventral node (vn, open arrow) between the ventral and the dorsal node, dn. Note that there is a single layer of FN protein at the basal surface of the node and the notochordal plate (spanning 1–2 confocal planes), while FN protein is present throughout the embryonic mesoderm, spanning the majority of the confocal planes through the embryo. Therefore, FN protein appears undetectable in the whole mount 3D view in panels C–C1. Scale bars are 100 μm, except in C1–2, scale bars are 50 μm.

such as Wnt, Shh, BMP4 and Fgf8 are among the key early features required for the development of the L–R axis in mammals (Caspary et al., 2007; Fischer et al., 2002; Meyers and Martin, 1999; Mine et al., 2008; Nakaya et al., 2005; Neugebauer et al., 2009; Tsukui et al., 1999). Therefore, we used SEM, whole mount *in situ* hybridization (ISH) and a TOPGAL reporter strain (DasGupta and Fuchs, 1999) to examine formation of the node, measure the length of nodal cilia, and assay growth factor expression and canonical Wnt signaling, respectively. Using expression of *Nodal* mRNA to mark the node and measuring the width of the node at its widest location, indicated that nodes in FN-null embryos were significantly narrower than in controls (Sup. Figs. 2A–D). This observation was also confirmed by

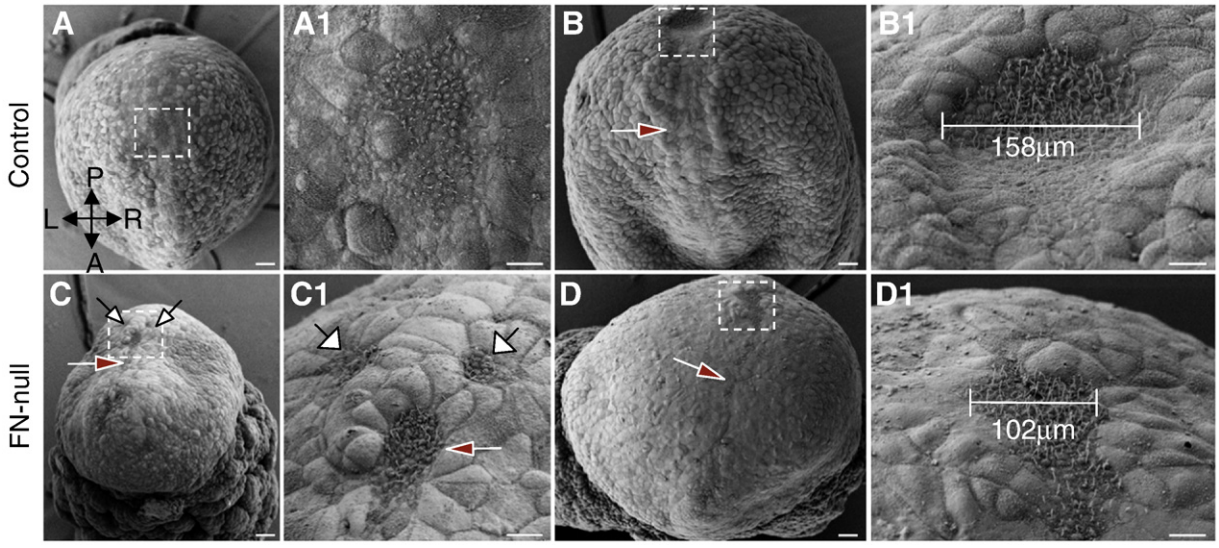


**Fig. 3.** FN is required for the morphogenesis of the node. A–B1. Control embryos. A. Early head fold (EHF) stage control embryo. B. E8.0, late head fold stage (LHF). C–D1. FN-null embryos (E8.0, LHF). A–A1. The node (located within the dashed box in A and expanded in A1) is composed of a nearly contiguous field of cells at E7.5. Some of the FN-null embryos (C–C1) contain discontinuous nodes, white arrows. By E8.0, control embryos (B–B1) contain a stereotypical nodal pit (boxed area) and notochordal plate (red arrow), while the node (boxed area) and the notochordal plate (red arrow) in FN-null embryos are narrow (D–D1). The nodes in FN-null embryos remain narrow at E8.5 (not shown). Magnifications are the same in panels A–D, scale bars are 30 μm. Boxes in A–D are expanded in A1–D1, scale bars are 10 μm. Axes are marked in panel A and are the same for all panels.

the SEM (Fig. 3). This defect was not due to a potential delay in the development of FN-nulls, compared with controls, since the width of the node was constant in groups of control embryos at the LHF stage, 0 somites, to 6 somites (Fig. 3 and Sup. Fig. 2D). Interestingly, the lengths of nodal cilia were similar in control (n = 4 embryos) and FN-null embryos (n = 4) indicating that FN is not required for the process of ciliogenesis (Sup. Figs. 2E–G). Moreover, since the length of the nodal cilia is particular to an embryonic stage of development (Lee and Anderson, 2008), similar lengths of cilia in FN-nulls and controls suggest that FN-null and control embryos analyzed in our studies were closely matched in age.

Our ISH analyses of growth factor expression showed that *Shh* mRNA is expressed in the nodes of FN-null embryos (Figs. 4C and D, black arrows) and the expression of *Ptch1*, an inhibitor and a positive indicator of Shh signaling (Goodrich et al., 1996), showed that FN is not required for Shh signaling in the node (Figs. 4E and F, black arrows). The overall expression patterns of *Fgf8* and *BMP4* mRNAs were also not significantly altered in FN-nulls (Sup. Fig. 5). Finally, we introduced a TOPGAL reporter allele into FN-null background, and observed the presence of β-gal activity within the narrow nodes of FN-null embryos, indicating that FN is not necessary for canonical Wnt signaling (data not shown). Taken in context with prior gene expression studies indicating that all examined embryonic precursors and lineages are specified in a grossly normal spatio-temporal pattern in FN-nulls (George et al., 1997; Georges-Labouesse et al., 1996; Mittal et al., 2010), our results emphasize that FN is particularly important for the development of the L–R axis of asymmetry.

Our studies suggested that FN plays an early role during the establishment of the L–R asymmetry by regulating the shape and the size of the mouse node. In order to understand why the nodes in FN-null mouse embryos are narrow, we used antibodies specific for the transcription factor FoxA2 and confocal fluorescence microscopy to visualize cells of the node and the notochordal plate (Fig. 5). These experiments showed the presence of multilayering of FoxA2-positive cells inside the node (in 6/7 FN-null embryos) and aberrant orientation of these cells within the nodes in FN-null embryos (Fig. 5B1), while in control embryos ranging from 0 (LHF stage) to 4 somites (n = 10), we have never observed multilayering of cells within the node (Fig. 5A1), and cells within the nodes of control embryos exhibited an organized and elongated orientation in all examined embryos (Fig. 5A1). These observations suggest that FN

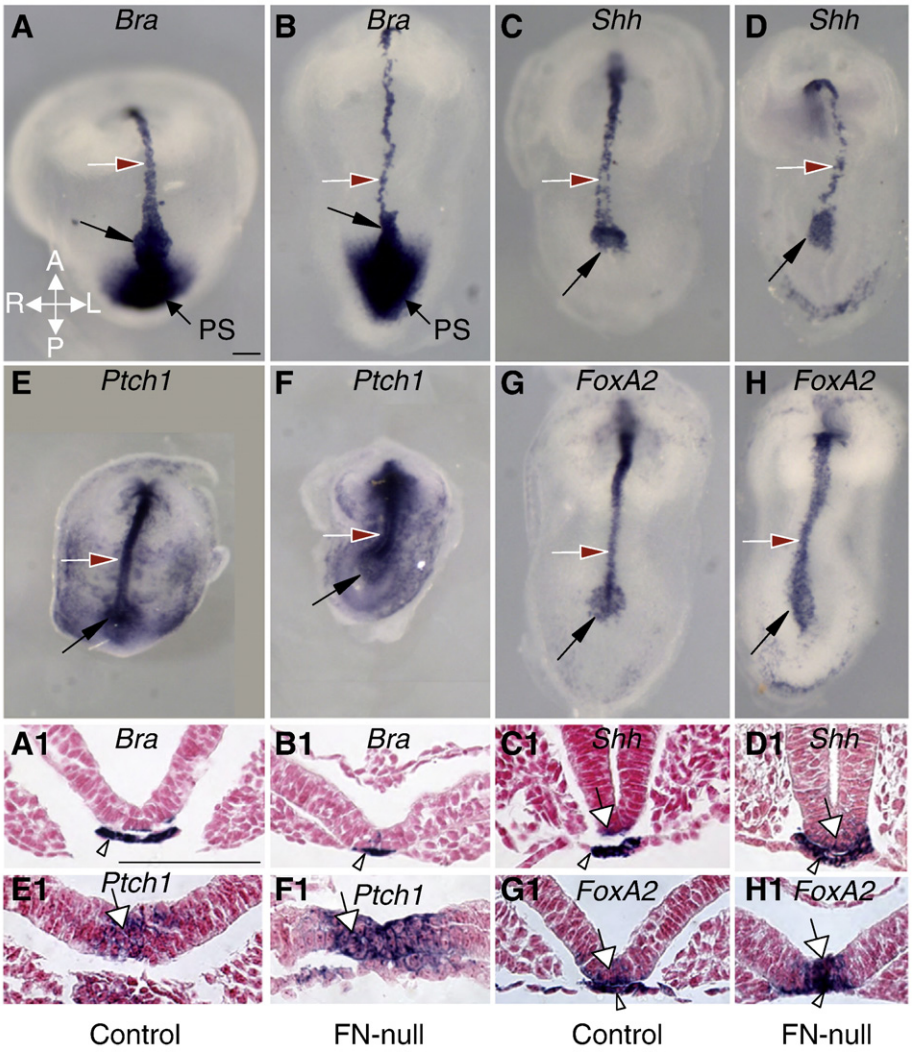


**Fig. 4.** FN is not required for the specification of cell fates in the node, notochord and the floor plate. A–H. Whole mount views of embryos stained by *in situ* hybridization detecting *Bra*, *Shh*, *Ptch1*, and *FoxA2* mRNAs, viewed ventrally. A1–H1. Transverse sections approximately at the levels indicated by the red arrows (except in C, D, the transverse sections were taken anterior to the foregut. A–B. *Bra*. Note thin notochordal plate in FN-null embryo (B). (C–H) *Shh, Ptch1* and *FoxA2* are expressed in the node (black arrows) and notochordal plate (red arrows) of control (C, E, G) and FN-null embryos (D, F, H). C1–H1. Transverse sections show that *Shh, Ptch1* and *FoxA2* are expressed in both the notochordal plate (arrowhead) and the floor plate (white arrow) in control and FN-nulls embryos. Dorsal is at the top and ventral is at the bottom in panels A1–H1. Magnifications are the same in panels A–H and in panels A1–H1. Scale bars are 100 μm.

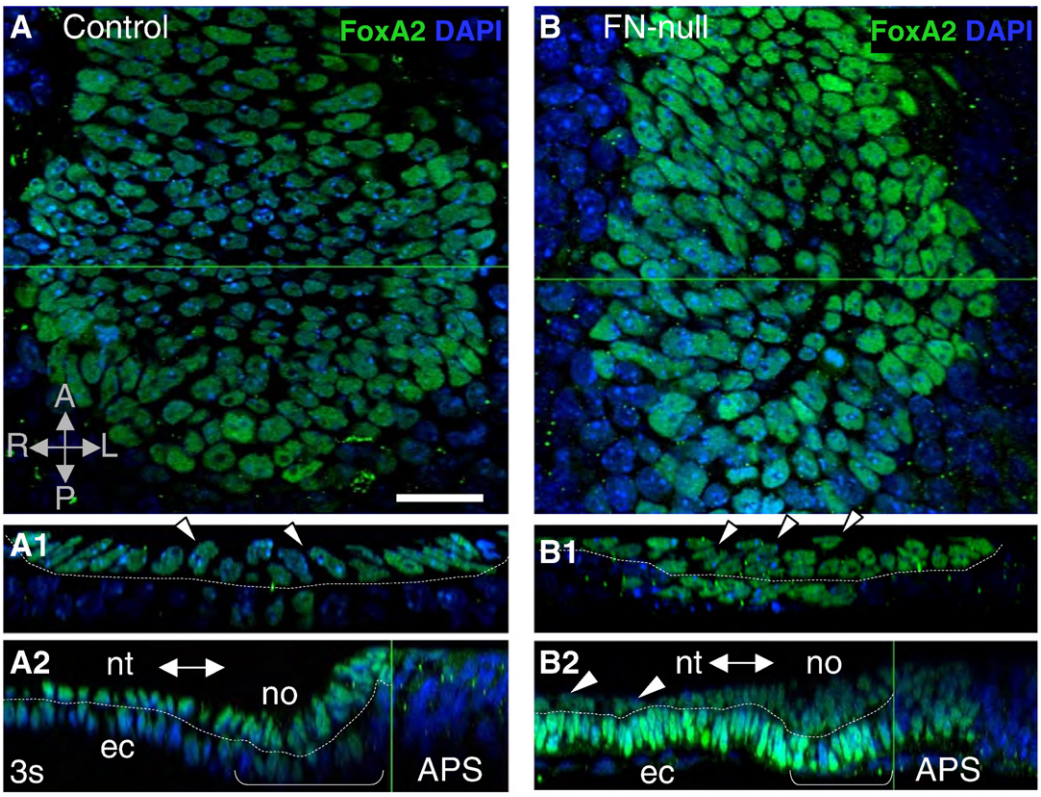


**Fig. 5.** FN is required for the morphogenesis of the two cell-layered structure of the ventral node. 3D reconstruction of confocal sections through the entire thickness of the node of a control, 3-somite embryo (A) and FN-null (B) embryo stained to detect FoxA2 protein (green) and nuclei (DAPI, blue). A1–B1. Orthogonal transverse confocal views (positions of the optical planes are shown in A and B, green line, through the nodes of the control and FN-null embryos. The dotted lines in A1–B1 mark the boundary between the ventral and the dorsal node. Ventral side is up and dorsal side is down in A1–B2. Cells within the node of control embryos are arranged in two layers and adapt elongated morphology (arrowheads). Cells within FN-null node are aberrantly oriented (arrowheads) relative to the ventral surface of the node and are arranged in multiple layers (B1). A2–B2. Orthogonal lengthwise confocal sections through the notochordal plate in the anterior (left) to posterior (right) direction, indicated by the double-headed arrow. Dashed lines in A2–B2 mark the border between the notochord (nt) and the neural ectoderm (ec); or the ventral node (no) and the dorsal node within the bracketed area. Notice the filled node and ectopic FoxA2 staining in the anterior primitive streak (APS) posterior to the node in FN-null (B2). Green lines in A2–B2 mark posterior borders of the node. Also note that some cells in the notochordal plate of FN-null embryo are oriented parallel to the ventral surface (arrowheads), while in control (A2), cells of the notochord are oriented perpendicular to the embryo's ventral surface. Magnification is the same in all panels, scale bar is 25 μm.

protein localized to the basal surface of the ventral node may be important for the proper orientation and vertical intercalation of nodal cells between each other, giving rise to the stereotypical, two-layered structure of the ventral node and leading to the expansion of the ventral surface area of the node, similar to the process of radial intercalation mediating BCR expansion in *Xenopus* (Marsden and DeSimone, 2001). Finally, we noticed that node(s) in 3/13 FN-null embryos were discontinuous, and in 6 out of 13 embryos, the nodes appeared flat instead of invaginated (Figs. 3C1 and D1), suggesting that formation of the nodal invagination is genetically controlled and that FN plays an important role in this process. Taken together, our data indicate that FN plays an essential early role during the establishment of the L–R body plan by regulating the morphogenesis of the contiguous, invaginated, two cell-layered structure of the mammalian node.

*Fibronectin is essential for the formation of the notochordal plate and the barrier function of the embryonic midline*

Establishment and maintenance of the L–R asymmetry in wild-type mammalian embryos is maintained through the barrier function of the embryonic midline, the notochordal plate and the prospective floor plate (Lohr et al., 1998; Meno et al., 1998; Nakamura et al., 2006; Oki et al., 2009). Using SEM and ISH, we observed that the notochordal plates were narrower and somewhat disrupted in the mutants compared with controls (Figs. 3B, D, and 4A–D). Interestingly, our ISH studies to evaluate the expression of *Bra*, *Shh*, *Ptch1*, and *FoxA2* mRNAs indicated that cell fates of notochordal precursors were specified in the absence of FN (Fig. 4). These findings are consistent with earlier studies (Georges-Labouesse et al., 1996) and indicate that while FN is not required for specification of notochordal cell fates or for Shh signaling, it is important for the notochordal morphogenesis. These observations suggest that in addition to the defective formation of the node, the aberrant orientation of the L–R axis could be also due to defective morphogenesis of the notochordal plate in FN-null embryos.

Both the establishment and the maintenance of the L–R axis of asymmetry depends on the expression of *Lefty1* in the floor plate (Oki et al., 2009). Expression of *Nodal* at the rim of the node induces expression of *Lefty1* in the midline within the node and the expression of *Lefty2* in the left LPM (Meno et al., 2001). Nodal protein produced in the left LPM can travel to the midline and induce the expression of *Lefty1* (and weakly, *Lefty2*) on the left side of the floor plate (Kumar et al., 2008; Marjoram and Wright, 2011; Ohi and Wright, 2007; Yamamoto et al., 2003). Lefty1 functions as an inhibitor of Nodal signaling (Sakuma et al., 2002) and its expression on the left side of the floor plate is thought to inhibit the passage of Nodal activity to the right LPM and/or to inhibit Nodal signaling at the right LPM (Meno et al., 1998). While we found that all examined FN-null embryos expressed *Shh*, *Ptch1* and *FoxA2* in the floor plate, we have not detected floor plate expression of *Lefty1/2* in the seven FN-nulls examined (e.g. Figs. 1G and H). The expression of *Shh*, *Ptch1* and *FoxA2* in the floor plate (Fig. 4) is the result of Shh signaling induced in the floor plate by the Shh protein produced by the notochordal plate

(Goodrich et al., 1996; Goodrich et al., 1997; Ribes et al., 2010; Tsukui et al., 1999). Our experiments thus indicate that while FN is not required for cell fate specification of the floor plate or for Shh signaling from the notochordal plate to the floor plate, it is essential for the induction of *Lefty1/2* at the midline.

FN protein is localized between the floor plate and the notochordal plate (Fig. 2C3) and presumably interacts and signals to the cells in its immediate vicinity. Cell adhesion to FN is known to facilitate growth factor signaling mediated by receptor tyrosine kinases (Giancotti and Tarone, 2003; Miyamoto et al., 1996). Since the expression of *Lefty1* in the midline could be induced by Nodal, we reasoned that the absence of *Lefty1/2* expression in the floor plate of FN-null embryos could be due to defective Nodal signaling at the midline in the absence of FN. Nodal belongs to the transforming growth factor (TGF) β family of proteins and signaling by this family of proteins results in phosphorylation of serines at the C-terminal SS(V/M)S motif of SMADs 2 and 3, activating these SMADs and leading to the formation of SMAD2/3–SMAD4 complexes. Upon translocation into the nucleus, these complexes can associate with FoxH1 and mediate gene transcription, leading to the expression of *Lefty1/2* (Massague, 1998; Sakuma et al., 2002). We noticed that activated forms of SMADs 2 and 3 were enriched at the midline of wild-type embryos with as few as 2 somites (Fig. 6, quantified in Sup. Fig. 3), which approximately corresponds with the time of the earliest induction of *Lefty1* at the floor plate (Mine et al., 2008). Analysis of transverse sections indicated that activated forms of pSMADs 2 and 3 are indeed enriched in the floor plate (Fig. 6A1, arrow pointing at the dark brown nuclei and Sup. Fig. 3). While in all of the control embryos (n = 8, ranging from 2 to 7 somites) the expression of activated forms of SMADs 2 and 3 were enriched at the floor plate, this enrichment was not detected in any of the FN-null embryos analyzed (n = 5) (e.g. Figs. 6B–C1 and quantified in Sup. Fig. 3). Interestingly, we observed the presence of active forms of these SMADs elsewhere in FN-null embryos, including the left LPM (Figs. 6B and C), and similar to controls, we observed enriched presence of active SMADs 2 and 3 in the left LPM of FN-nulls (Fig. 6B, white arrowhead), suggesting that FN is not required to facilitate Nodal signaling in the LPM in contrast with the floor plate. While we do not currently understand the basis for this difference, it is known that asymmetric expression patterns of *Lefty1* and *Lefty2* are regulated by distinct genetic elements and mechanisms (Saijoh et al., 1999), and that Nodal activity gives rise to distinct transcriptional responses in distinct embryonic locations, e.g. anterior left LPM compared with posterior left LPM and the floor plate (Meno et al., 2001; Yamamoto et al., 2001). We also cannot rule out the possibility that higher threshold levels of Nodal activity are needed to activate SMAD 2/3 signaling in the floor plate compared with the LPM in the absence of FN. Since cellular fates in the floor plate are specified, our data suggests a possibility that FN specifically regulates the expression of *Lefty1/2* by regulating Nodal signaling and activation of SMADs 2/3 at the floor plate.

### *Conserved requirement for integrin α5 in the development of the L–R asymmetry*

In order to uncover mechanisms whereby FN functions to establish L–R axis, we asked whether integrin α5 were also essential for the development of the embryonic L–R axis. To answer this question, we examined the expression of *Nodal, Lefty1, 2* and *Pitx2c* mRNAs in integrin α5-null and control embryos, and similar to FN, we found that the expression of these genes in the LPM was no longer confined to the left side in integrin α5-null embryos (Figs. 7E–M). Because integrin α5-null embryos develop further than FN-nulls, we were able to assess cardiac looping in these mutants. In wild-type embryos, the heart loops to the right, and this event is the first sign of the morphological L–R asymmetry in a developing vertebrate embryo (Shiratori and Hamada, 2006). We found that while in 1/15 examined integrin α5-null embryos, heart indeed looped to the right, in 5/15 integrin α5-null embryos heart looped to the left. The remaining mutants contained straight heart tubes situated along the midline (Figs. 7A–C). These observations indicate that integrin α5 is required

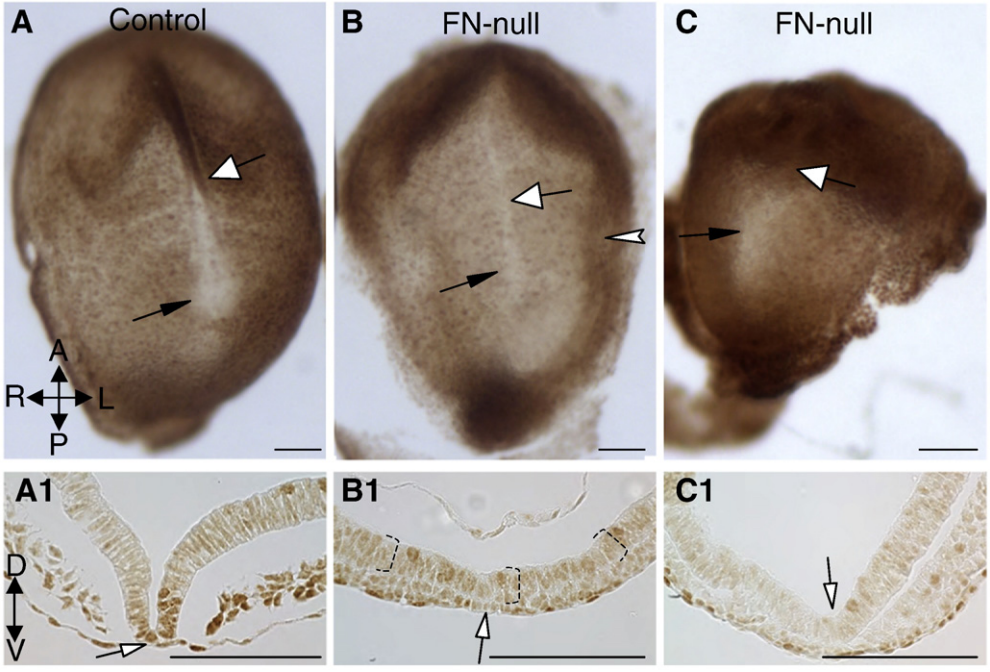


**Fig. 6.** FN is required for the expression of activated forms of SMADs 2 and 3 at the midline. A. Control and FN-null embryos (B, C) stained to detect activated forms of SMADs 2 and 3. Black arrows point at the nodes and white arrows point at the midline and indicate the approximate levels of transverse sections in A1–C1. The presence of activated pSMADs 2 and 3 is enriched in the floor plate (white-filled arrows) of control embryo (dark brown nuclei). Notice decreased levels of activated pSMADs 2/3 at the midline and the floor plate of FN-null embryos (B–C1). Dotted brackets in B1 mark neural ectoderm. Magnification is the same in panels A–C and A1–C1. All scale bars are 100 μm.

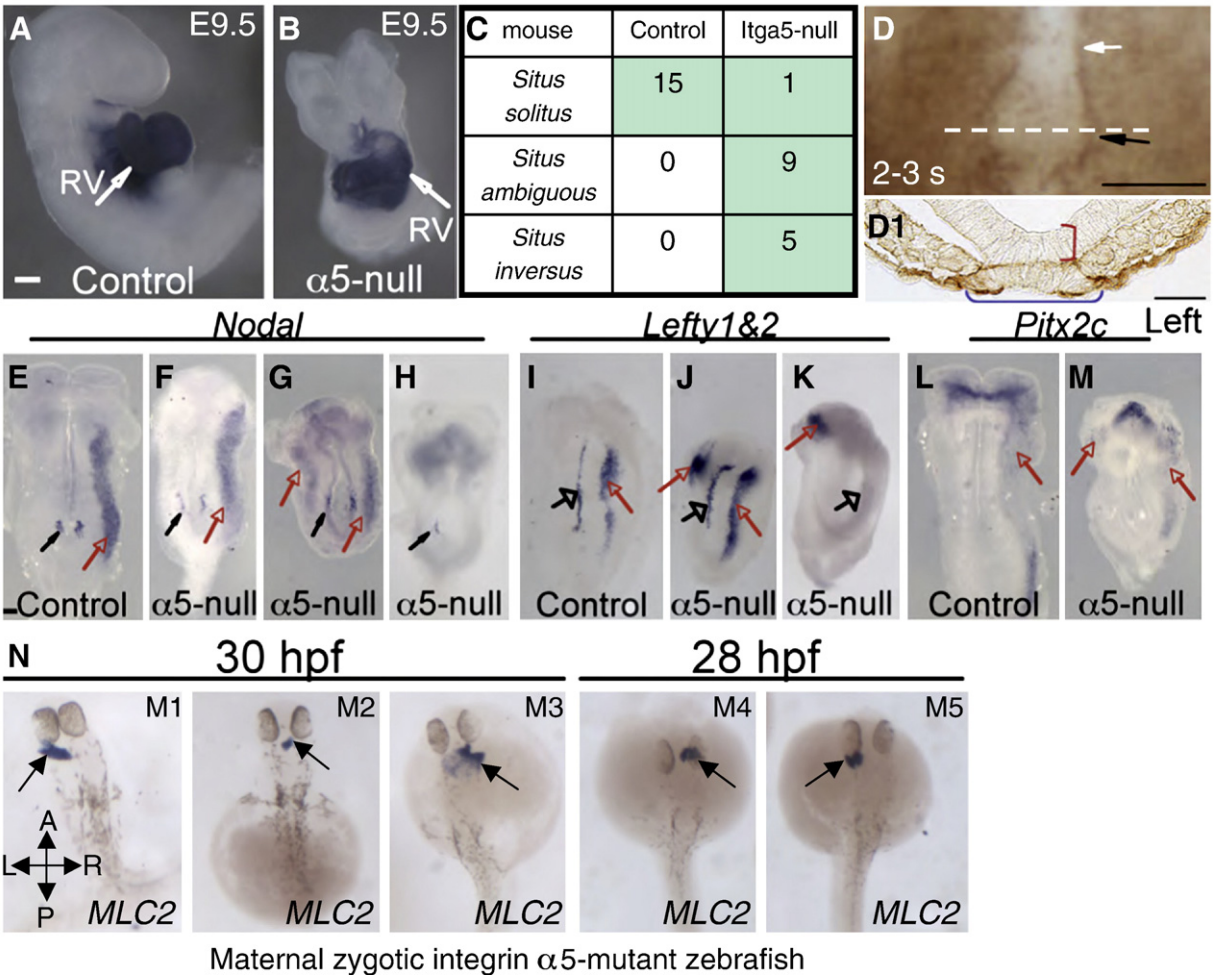


Maternal zygotic integrin α5-mutant zebrafish

**Fig. 7.** Integrin α5 is required for normal cardiac morphogenesis in mice and fish, and the asymmetric expression of *Nodal*, *Lefty* and *Pitx2c*. Normal rightward looping of the heart in a control embryo (A, right side view), and reversed leftward looping of the heart in an integrin α5-null embryo (B, ventral view), the hearts are visualized by ISH with Nkx2.5 probe, and the cardiac looping phenotypes are summarized in the table (C). RV—right ventricle. D. Expression of integrin α5 protein (brown) around the node, black arrow and the notochordal plate, white arrow. Staining with control, rat IgG, resulted only in a faint, non-distinct background (data not shown). Ventral view is shown, axes are as in Fig. 1A. D1. Transverse section through the node of the embryo (dotted line in D), showing the localization of integrin α5 to the basal surface of embryonic and visceral endoderm, and basal surface of the ventral node marked by the blue horizontal bracket. Red vertical bracket marks the dorsal node. E–H. *Nodal* mRNA. I–K. *Lefty1* and *2* mRNA. L, M. *Pitx2c* mRNA. E–M. All views are ventral, the axes are as in Fig. 1A. Black arrows point at the nodes, red arrows point at the LPM, open arrows point at the midline in I–K. N. Dorsal views of maternal-zygotic integrin α5-null zebrafish mutants stained using *in situ* hybridization to detect *MLC2*. Axes are marked in panel M1. Examples of a normal leftward displacement of the heart (M1) and abnormal heart morphogenesis are shown in M2–5. M2. Heart tube is moved to the right. M3. *Cardia bifida*, in which both heart primordia moved to the right. M4. *Cardia bifida* where cardiac primordia are located to the right of the midline. M5. *Cardia bifida* where the cardiac primordia are located to the left of the midline. Magnifications are the same in all panels. In all control embryos (n = 16) a single heart tube was formed and moved to the left by 24 hpf (not shown). Magnifications are the same in A–B, in E–M, and N. All scale bars are 100 μm, except in D1 the scale bar is 25 μm.

for the L–R specific gene expression and for the development of the morphological L–R asymmetry.

To test the hypothesis that the requirement for integrin α5 in the development of L–R asymmetry is evolutionarily conserved in vertebrates, we analyzed the position of the heart in maternal-zygotic integrin α5-null zebrafish (Fig. 7N). By 24 hours post fertilization (hpf), zebrafish heart jogs to the left, giving rise to the asymmetrically positioned heart tube relative to the midline (Yelon, 2001). Analysis of integrin α5-null maternal-zygotic mutants (Julich et al., 2005) using ISH to detect cardiac myosin light chain 2 (*cmlc2*) expression, indicated that in 4 out of 37 mutant embryos hearts moved to the right. In 11/37 mutants, heart tubes remained positioned along the midline, and in 22/37 mutants, hearts moved to the left (Fig. 7N), while in all analyzed control zebrafish embryos (n = 16), heart tubes moved to the left (data not shown). These data indicate an evolutionarily conserved requirement for integrin α5 during the development of the L–R body plan in vertebrates and suggest that some functions of FN during the development of L–R asymmetry are mediated by integrin α5β1.

## Discussion

Our studies demonstrated that FN, an essential component of the ECM, is necessary for the development of the stereotypical L–R asymmetric gene expression pattern requisite for asymmetrical organ morphogenesis. FN protein is expressed around the ventral node and the notochordal plate, and we observed that nodes of FN-null embryos were narrow and discontinuous. However, nodal cilia lengths were comparable between the null and control embryos; each nodal cell observable by SEM contained one cilium and cilia were properly positioned at the posterior ends of cells within the node in the mutants. These observations suggest that FN is not required for ciliogenesis or to impart anterior–posterior polarity to cells of the node. Cells within the nodes of FN-null embryos formed multiple layers of aberrantly oriented cells, while in wild-type embryos the ventral node is composed of a regular array of cells that are elongated in a roughly dorsal-to-ventral direction. These observations suggest that FN is required for the proper orientation of nodal cells within the node, probably by imparting ventral-to-dorsal (apico-basal) polarity

to the cells and for the vertical intercalation of nodal cells between each other to generate the stereotypical, two cell-layered structure of the nodal pit. While we cannot completely exclude the possibility of abnormal nodal flow in FN-nulls, we speculate that the initial requirement for FN during establishment of L–R body plan is in mediating morphogenesis of the node.

Morphogenesis of the node is a complex process, during which cells of the future node emerge on the embryonic ventral surface by intercalating between the visceral endodermal cells covering the embryo (Lee and Anderson, 2008; Lee et al., 2010; Sulik et al., 1994). When the ventral surfaces of mammalian embryos at the early head fold stage are observed by confocal fluorescence microscopy, the node appears as a stream of connected islands, before it adopts its canonical tear-drop shape, presumably due to assembly of the islands of nodal cells into the stereotypical structure of the node (Lee and Anderson, 2008). However, the nodal islands in 3 out of 13 FN-nulls were not connected to each other, instead, they were separated by large cells of the visceral endoderm, a morphogenetic defect very similar to that found in *lulu* mutants, a null mutation in the gene encoding *Epb4.1l5* (Lee et al., 2010; Lee et al., 2007). In addition, the nodes in 6 out of 13 FN-null embryos appeared flat when observed using SEM. These observations suggest that FN could be important at several stages during morphogenesis of the ventral node: 1) it could facilitate intercalation of nodal cells initially located underneath the embryonic surface with the cells of the visceral endoderm (Lee et al., 2010; Sulik et al., 1994); 2) facilitate intercalation of nodal cells with each other, giving rise to the expanded nodal structure, analogous to the role of FN in radial intercalation of cells of the blastocoel roof during epiboly in *Xenopus* (Marsden and DeSimone, 2001); 3) facilitate assembly of the final shape of the node from populations of nodal cells by regulating the cohesiveness between the cells of the nascent node. Indeed, studies in *Xenopus* indicated that cell–matrix adhesion to FN regulates cell–cell adhesion and sorting behavior of cells possibly by regulating the activation state of cadherins (Marsden and DeSimone, 2003); 4) FN may participate in the formation of the invaginated nodal structure by regulating apico-basal polarity, analogous to the role of ECM and integrins during formation of vascular lumens (Davis et al., 2007; Zovein et al., 2010).

FN is a large and complex glycoprotein composed of multiple domains (Hynes, 1990). While we do not currently understand which domain or a combination of domains of FN is (are) required for the establishment of L–R asymmetry, we note that mice lacking both EIIIA and EIIIB alternatively spliced variants of FN do not develop L–R defects (Astrof et al., 2007a). To begin understanding the signaling pathways downstream of FN, we investigated the role of integrin α5 in L–R morphogenesis and found that it is required for the stereotypical, asymmetric gene expression in mice and for the proper asymmetric positioning of the heart in mice and fish, indicating a conserved requirement for integrin α5 in L–R development in vertebrates. Interestingly, the phenotype of integrin α5-null L–R defects is not entirely the same as that of FN-nulls. Similar to FN-nulls, the nodes of integrin α5-null embryos are flat and in some embryos, contain aberrantly oriented cells, however the nodes in integrin α5-null mutants are nearly 40% wider than in controls ($p<10^{-6}$, Student's t test) (M.P. and S.A. unpublished, in preparation). The differences in the phenotypes of FN-null and integrin α5-null embryos could be due to compensatory or overlapping functions of other FN-binding integrins—likely mediated by the αv-containing integrin heterodimers, αvβ1, αvβ3 or αvβ5 (Yang et al., 1999; Yang and Hynes, 1996). This is because the concurrent deletion of integrin αv and α5 genes gives rise to a phenotype that is much more severe than the individual deletion of each of these integrins, while the simultaneous deletion of other FN-binding integrins such as α4 and α5, eliminating three different integrin heterodimers (α4β1, α4β7 and α5β1), or α3 and α5, gave rise to mutant embryos with phenotypes resembling α5-nulls. Deletion of α3 and α4 integrins in mice resulted in α4-null like phenotype, which is both milder and different than the deletion of integrin α5 alone (Yang et al., 1999; Yang et al., 1995). Interestingly, recent studies in fish demonstrated that integrins containing αv and/or β1d subunits were expressed in the dorsal forerunner cells (DFC) and were required for the morphogenesis of the Kupffer's vesicle (KV), an organ of asymmetry in zebrafish (Ablooglu et al., 2010; Essner et al., 2005). In these mutants, the spherical shape characteristic of the KV was distorted and instead of one intact KV, the KV in the mutants was often present in the form of patches of DFCs. This phenotype is similar to the phenotype of FN-null embryos, in which patches of nodal cells are sometimes observed on embryonic surface instead of one contiguous node. Therefore, it is possible that integrins containing αv and α5 subunits could perform overlapping or complementary functions during node morphogenesis in the mouse. Future studies investigating the individual and combined functions of these integrins during early embryonic development would provide further insight into the role of cell-matrix adhesion in node morphogenesis.

Our experiments also demonstrated the requisite role of FN during morphogenesis of the notochordal plate. While the cell fate of the notochordal precursors is specified in the absence of FN, as judged by the expression of *Shh*, *Patched1*, *Brachyury* and *FoxA2*, this structure appeared narrow by SEM and seemed interrupted when visualized using ISH. The narrowness of and discontinuities in the notochordal plate in FN-nulls could also contribute to the defective L–R axis development in these mutants. Interestingly, we found that the function of the notochordal plate as a signaling center was not significantly disrupted by the absence of FN. Indeed Shh signaling by the notochordal plate to itself and to the prospective floor plate was not disturbed as judged by the expression of genes known to be induced by Shh, *Patched1* and *FoxA2*. Similarly, the function of the floor plate as a signaling center was not disrupted either, since we observed the expression of *Shh*, *Patched1* and *FoxA2* in the ventral cells of the neural ectoderm, indicating that Shh signaling to and within the floor plate is functional in the absence of FN. Moreover, we consistently noted a more extensive expression of *Patched1* and *FoxA2* mRNAs in the axial structures of FN-null embryos compared with controls (Figs. 4E1–H1). In addition, the expression of FoxA2 protein is also more extensive in FN-null embryos and is no longer confined just to the floor plate of the neural ectoderm (Figs. 5A2–B2) but spreads more dorsally, suggesting an increase in Shh signaling and spread. Both *Patched1* and *FoxA2* mRNAs in the floor plate are induced as a response to Shh signaling emanating from the notochordal plate. We speculate that the presence of FN protein between the notochordal plate and the ventral surface of the neural ectoderm (the floor plate) limits diffusion of Shh protein and/or signaling by Shh from the notochord to the floor plate.

Even though cell fate and signaling functions of the midline were preserved in FN-null mutants, we did not detect expression of *Lefty1* and *2* mRNAs in the floor plate (the probe used in these ISH experiments detects transcripts of both genes). This was likely due to the downregulation of Nodal signaling to the floor plate in FN-null embryos, since the enrichment of activated SMADs 2 and 3 in the floor plate was undetectable in the absence of FN. There are several possible reasons for the lower levels of these activated SMADs at the midline of FN-null mutants, such as potentially lower levels of Nodal activity reaching the midline or defective signaling by Nodal protein to the cells of the floor plate in the absence of FN. These possibilities will be addressed in the future. Taken together, our studies demonstrated the requisite role of FN and integrin α5 in the development of the L–R axis of asymmetry.

Supplementary materials related to this article can be found online at doi:10.1016/j.ydbio.2011.03.026.

## Acknowledgments

We thank Nina Lampen at the Electron Microscopy Core Facility at the Memorial Sloan-Kettering Cancer Center for help with SEM,

Shivaprasad Bhuvanendran in the Bio-Imaging Resource Center at the Rockefeller University for help with confocal imaging, Dr. Yutaka Nibu for the use of his microscope and imaging equipment, Dr. Todd Evans and Amir Raikin for advice on zebrafish staining. We thank Kat Hadjantonakis and Chris Wright for insightful discussions and critical reading of the manuscript, Glenn Radice, Xia Wang, Nathan Astrof for critical reading of the manuscript, and Margit Neszmelyi for editorial assistance. This work was supported by the start up funds to S.A. from the Division of Cardiology at Weill Cornell Medical College and by the American Heart Association Scientist Development grant # 0835556D to S.A.

## References

Ablooglu, A.J., Tkachenko, E., Kang, J., Shattil, S.J., 2010. Integrin alphaV is necessary for gastrulation movements that regulate vertebrate body asymmetry. Development 137, 3449–3458.

Amack, J.D., Wang, X., Yost, H.J., 2007. Two T-box genes play independent and cooperative roles to regulate morphogenesis of ciliated Kupffer's vesicle in zebrafish. Dev. Biol. 310, 196–210.

Astrof, S., Crowley, D., Hynes, R.O., 2007a. Multiple cardiovascular defects caused by the absence of alternatively spliced segments of fibronectin. Dev. Biol. 311, 11–24.

Astrof, S., Kirby, A., Lindblad-Toh, K., Daly, M., Hynes, R.O., 2007b. Heart development in fibronectin-null mice is governed by a genetic modifier on chromosome four. Mech. Dev. 124, 551–558.

Bader, B.L., Rayburn, H., Crowley, D., Hynes, R.O., 1998. Extensive vasculogenesis, angiogenesis, and organogenesis precede lethality in mice lacking all alpha v integrins. Cell 95, 507–519.

Bamford, R.N., Roessler, E., Burdine, R.D., Saplakoglu, U., dela Cruz, J., Splitt, M., Goodship, J.A., Towbin, J., Bowers, P., Ferrero, G.B., et al., 2000. Loss-of-function mutations in the EGF–CFC gene CFC1 are associated with human left–right laterality defects. Nat. Genet. 26, 365–369.

Brennan, J., Norris, D.P., Robertson, E.J., 2002. Nodal activity in the node governs left–right asymmetry. Genes Dev. 16, 2339–2344.

Caspary, T., Larkins, C.E., Anderson, K.V., 2007. The graded response to Sonic Hedgehog depends on cilia architecture. Dev. Cell 12, 767–778.

Chan, C.S., Chen, H., Bradley, A., Dragatsis, I., Rosenmund, C., Davis, R.L., 2010. Alpha8-integrins are required for hippocampal long-term potentiation but not for hippocampal-dependent learning. Genes Brain Behav. 9, 402–410.

DasGupta, R., Fuchs, E., 1999. Multiple roles for activated LEF/TCF transcription complexes during hair follicle development and differentiation. Development 126, 4557–4568.

Davidson, L.A., Hoffstrom, B.G., Keller, R., DeSimone, D.W., 2002. Mesendoderm extension and mantle closure in *Xenopus laevis* gastrulation: combined roles for integrin alpha(5)beta(1), fibronectin, and tissue geometry. Dev. Biol. 242, 109–129.

Davidson, L.A., Marsden, M., Keller, R., Desimone, D.W., 2006. Integrin alpha5beta1 and fibronectin regulate polarized cell protrusions required for *Xenopus* convergence and extension. Curr. Biol. 16, 833–844.

Davidson, L.A., Dzamba, B.D., Keller, R., Desimone, D.W., 2008. Live imaging of cell protrusive activity, and extracellular matrix assembly and remodeling during morphogenesis in the frog, *Xenopus laevis*. Dev. Dyn. 237, 2684–2692.

Davis, G.E., Koh, W., Stratman, A.N., 2007. Mechanisms controlling human endothelial lumen formation and tube assembly in three-dimensional extracellular matrices. Birth Defects Res. C Embryo Today 81, 270–285.

Downs, K.M., Davies, T., 1993. Staging of gastrulating mouse embryos by morphological landmarks in the dissecting microscope. Development 118, 1255–1266.

Essner, J.J., Amack, J.D., Nyholm, M.K., Harris, E.B., Yost, H.J., 2005. Kupffer's vesicle is a ciliated organ of asymmetry in the zebrafish embryo that initiates left–right development of the brain, heart and gut. Development 132, 1247–1260.

Fassler, R., Meyer, M., 1995. Consequences of lack of beta 1 integrin gene expression in mice. Genes Dev. 9, 1896–1908.

Fischer, A., Viebahn, C., Blum, M., 2002. FGF8 acts as a right determinant during establishment of the left–right axis in the rabbit. Curr. Biol. 12, 1807–1816.

George, E.L., Georges-Labouesse, E.N., Patel-King, R.S., Rayburn, H., Hynes, R.O., 1993. Defects in mesoderm, neural tube and vascular development in mouse embryos lacking fibronectin. Development 119, 1079–1091.

George, E.L., Baldwin, H.S., Hynes, R.O., 1997. Fibronectins are essential for heart and blood vessel morphogenesis but are dispensable for initial specification of precursor cells. Blood 90, 3073–3081.

Georges-Labouesse, E.N., George, E.L., Rayburn, H., Hynes, R.O., 1996. Mesodermal development in mouse embryos mutant for fibronectin. Dev. Dyn. 207, 145–156.

Giancotti, F.G., Tarone, G., 2003. Positional control of cell fate through joint integrin/receptor protein kinase signaling. Annu. Rev. Cell Dev. Biol. 19, 173–206.

Goodrich, L.V., Johnson, R.L., Milenkovic, L., McMahon, J.A., Scott, M.P., 1996. Conservation of the hedgehog/patched signaling pathway from flies to mice: induction of a mouse patched gene by Hedgehog. Genes Dev. 10, 301–312.

Goodrich, L.V., Milenkovic, L., Higgins, K.M., Scott, M.P., 1997. Altered neural cell fates and medulloblastoma in mouse patched mutants. Science 277, 1109–1113.

Grande, C., Patel, N.H., 2009. Nodal signalling is involved in left–right asymmetry in snails. Nature 457, 1007–1011.

Henrique, D., Adam, J., Myat, A., Chitnis, A., Lewis, J., Ish-Horowicz, D., 1995. Expression of a Delta homologue in prospective neurons in the chick. Nature 375, 787–790.

Hynes, R.O., 1990. Fibronectins. Springer-Verlag, New York.

Hynes, R.O., 2002. Integrins: bidirectional, allosteric signaling machines. Cell 110, 673–687.

Julich, D., Geisler, R., Holley, S.A., 2005. Integrinalpha5 and delta/notch signaling have complementary spatiotemporal requirements during zebrafish somitogenesis. Dev. Cell 8, 575–586.

Julich, D., Mould, A.P., Koper, E., Holley, S.A., 2009. Control of extracellular matrix assembly along tissue boundaries via Integrin and Eph/Ephrin signaling. Development 136, 2913–2921.

Kinder, S.J., Tsang, T.E., Wakamiya, M., Sasaki, H., Behringer, R.R., Nagy, A., Tam, P.P., 2001. The organizer of the mouse gastrula is composed of a dynamic population of progenitor cells for the axial mesoderm. Development 128, 3623–3634.

Klass, C.M., Couchman, J.R., Woods, A., 2000. Control of extracellular matrix assembly by syndecan-2 proteoglycan. J. Cell Sci. 113 (Pt 3), 493–506.

Kramer, K.L., Yost, H.J., 2002. Ectodermal syndecan-2 mediates left–right axis formation in migrating mesoderm as a cell-nonautonomous Vg1 cofactor. Dev. Cell 2, 115–124.

Kumar, A., Lualdi, M., Lewandoski, M., Kuehn, M.R., 2008. Broad mesodermal and endodermal deletion of Nodal at postgastrulation stages results solely in left/right axial defects. Dev. Dyn. 237, 3591–3601.

Kwon, G.S., Viotti, M., Hadjantonakis, A.K., 2008. The endoderm of the mouse embryo arises by dynamic widespread intercalation of embryonic and extraembryonic lineages. Dev. Cell 15, 509–520.

Lee, J.D., Anderson, K.V., 2008. Morphogenesis of the node and notochord: the cellular basis for the establishment and maintenance of left–right asymmetry in the mouse. Dev. Dyn. 237, 3464–3476.

Lee, J.D., Silva-Gagliardi, N.F., Tepass, U., McGlade, C.J., Anderson, K.V., 2007. The FERM protein Epb4.1l5 is required for organization of the neural plate and for the epithelial-mesenchymal transition at the primitive streak of the mouse embryo. Development 134, 2007–2016.

Lee, J.D., Migeotte, I., Anderson, K.V., 2010. Left–right patterning in the mouse requires Epb4.1l5-dependent morphogenesis of the node and midline. Dev. Biol. 346, 237–246.

Levin, M., Johnson, R.L., Stern, C.D., Kuehn, M., Tabin, C., 1995. A molecular pathway determining left–right asymmetry in chick embryogenesis. Cell 82, 803–814.

Lohr, J.L., Danos, M.C., Groth, T.W., Yost, H.J., 1998. Maintenance of asymmetric nodal expression in *Xenopus laevis*. Dev. Genet. 23, 194–202.

Marjoram, L., Wright, C., 2011. Rapid differential transport of Nodal and Lefty on sulfated proteoglycan-rich extracellular matrix regulates left–right asymmetry in Xenopus. Development 138, 475–485.

Marsden, M., DeSimone, D.W., 2001. Regulation of cell polarity, radial intercalation and epiboly in *Xenopus*: novel roles for integrin and fibronectin. Development 128, 3635–3647.

Marsden, M., DeSimone, D.W., 2003. Integrin-ECM interactions regulate cadherin-dependent cell adhesion and are required for convergent extension in Xenopus. Curr. Biol. 13, 1182–1191.

Massague, J., 1998. TGF-beta signal transduction. Annu. Rev. Biochem. 67, 753–791.

Meno, C., Shimono, A., Saijoh, Y., Yashiro, K., Mochida, K., Ohishi, S., Noji, S., Kondoh, H., Hamada, H., 1998. Lefty-1 is required for left–right determination as a regulator of lefty-2 and nodal. Cell 94, 287–297.

Meno, C., Takeuchi, J., Sakuma, R., Koshiba-Takeuchi, K., Ohishi, S., Saijoh, Y., Miyazaki, J., ten Dijke, P., Ogura, T., Hamada, H., 2001. Diffusion of nodal signaling activity in the absence of the feedback inhibitor Lefty2. Dev. Cell 1, 127–138.

Meyers, E.N., Martin, G.R., 1999. Differences in left–right axis pathways in mouse and chick: functions of FGF8 and SHH. Science 285, 403–406.

Mine, N., Anderson, R.M., Klingensmith, J., 2008. BMP antagonism is required in both the node and lateral plate mesoderm for mammalian left–right axis establishment. Development 135, 2425–2434.

Mittal, A., Pulina, M., Hou, S.Y., Astrof, S., 2010. Fibronectin and integrin alpha 5 play essential roles in the development of the cardiac neural crest. Mech. Dev. 127, 472–484.

Miyamoto, S., Teramoto, H., Gutkind, J.S., Yamada, K.M., 1996. Integrins can collaborate with growth factors for phosphorylation of receptor tyrosine kinases and MAP kinase activation: roles of integrin aggregation and occupancy of receptors. J. Cell Biol. 135, 1633–1642.

Nakamura, T., Mine, N., Nakaguchi, E., Mochizuki, A., Yamamoto, M., Yashiro, K., Meno, C., Hamada, H., 2006. Generation of robust left–right asymmetry in the mouse embryo requires a self-enhancement and lateral-inhibition system. Dev. Cell 11, 495–504.

Nakaya, M.A., Biris, K., Tsukiyama, T., Jaime, S., Rawls, J.A., Yamaguchi, T.P., 2005. Wnt3a links left–right determination with segmentation and anteroposterior axis elongation. Development 132, 5425–5436.

Neugebauer, J.M., Amack, J.D., Peterson, A.G., Bisgrove, B.W., Yost, H.J., 2009. FGF signalling during embryo development regulates cilia length in diverse epithelia. Nature 458, 651–654.

Nonaka, S., Shiratori, H., Saijoh, Y., Hamada, H., 2002. Determination of left–right patterning of the mouse embryo by artificial nodal flow. Nature 418, 96–99.

Norris, D.P., Brennan, J., Bikoff, E.K., Robertson, E.J., 2002. The Foxh1-dependent autoregulatory enhancer controls the level of Nodal signals in the mouse embryo. Development 129, 3455–3468.

Oh, S.P., Li, E., 1997. The signaling pathway mediated by the type IIB activin receptor controls axial patterning and lateral asymmetry in the mouse. Genes Dev. 11, 1812–1826.

Ohashi, T., Kiehart, D.P., Erickson, H.P., 1999. Dynamics and elasticity of the fibronectin matrix in living cell culture visualized by fibronectin-green fluorescent protein. Proc. Natl Acad. Sci. U. S. A. 96, 2153–2158.

Ohi, Y., Wright, C.V., 2007. Anteriorward shifting of asymmetric Xnr1 expression and contralateral communication in left–right specification in Xenopus. Dev. Biol. 301, 447–463.

Oki, S., Kitajima, K., Marques, S., Belo, J.A., Yokoyama, T., Hamada, H., Meno, C., 2009. Reversal of left–right asymmetry induced by aberrant Nodal signaling in the node of mouse embryos. Development 136, 3917–3925.

Ramsdell, A.F., 2005. Left–right asymmetry and congenital cardiac defects: getting to the heart of the matter in vertebrate left–right axis determination. Dev. Biol. 288, 1–20.

Ribes, V., Balaskas, N., Sasai, N., Cruz, C., Dessaud, E., Cayuso, J., Tozer, S., Yang, L.L., Novitch, B., Marti, E., et al., 2010. Distinct Sonic Hedgehog signaling dynamics specify floor plate and ventral neuronal progenitors in the vertebrate neural tube. Genes Dev. 24, 1186–1200.

Saijoh, Y., Adachi, H., Mochida, K., Ohishi, S., Hirao, A., Hamada, H., 1999. Distinct transcriptional regulatory mechanisms underlie left–right asymmetric expression of lefty-1 and lefty-2. Genes Dev. 13, 259–269.

Saijoh, Y., Adachi, H., Sakuma, R., Yeo, C.Y., Yashiro, K., Watanabe, M., Hashiguchi, H., Mochida, K., Ohishi, S., Kawabata, M., et al., 2000. Left–right asymmetric expression of lefty2 and nodal is induced by a signaling pathway that includes the transcription factor FAST2. Mol. Cell 5, 35–47.

Sakuma, R., Ohnishi Yi, Y., Meno, C., Fujii, H., Juan, H., Takeuchi, J., Ogura, T., Li, E., Miyazono, K., Hamada, H., 2002. Inhibition of Nodal signalling by Lefty mediated through interaction with common receptors and efficient diffusion. Genes Cells 7, 401–412.

Saoncella, S., Echtermeyer, F., Denhez, F., Nowlen, J.K., Mosher, D.F., Robinson, S.D., Hynes, R.O., Goetinck, P.F., 1999. Syndecan-4 signals cooperatively with integrins in a Rho-dependent manner in the assembly of focal adhesions and actin stress fibers. Proc. Natl Acad. Sci. U. S. A. 96, 2805–2810.

Shiratori, H., Hamada, H., 2006. The left–right axis in the mouse: from origin to morphology. Development 133, 2095–2104.

Sulik, K., Dehart, D.B., Iangaki, T., Carson, J.L., Vrablic, T., Gesteland, K., Schoenwolf, G.C., 1994. Morphogenesis of the murine node and notochordal plate. Dev. Dyn. 201, 260–278.

Takahashi, S., Leiss, M., Moser, M., Ohashi, T., Kitao, T., Heckmann, D., Pfeifer, A., Kessler, H., Takagi, J., Erickson, H.P., et al., 2007. The RGD motif in fibronectin is essential for development but dispensable for fibril assembly. J. Cell Biol. 178, 167–178.

Trinh, L.A., Stainier, D.Y., 2004. Fibronectin regulates epithelial organization during myocardial migration in zebrafish. Dev. Cell 6, 371–382.

Tsukui, T., Capdevila, J., Tamura, K., Ruiz-Lozano, P., Rodriguez-Esteban, C., Yonei-Tamura, S., Magallon, J., Chandraratna, R.A., Chien, K., Blumberg, B., et al., 1999. Multiple left–right asymmetry defects in Shh(−/−) mutant mice unveil a convergence of the shh and retinoic acid pathways in the control of Lefty-1. Proc. Natl Acad. Sci. U. S. A. 96, 11376–11381.

van der Flier, A., Sonnenberg, A., 2001. Function and interactions of integrins. Cell Tissue Res. 305, 285–298.

Yamamoto, M., Meno, C., Sakai, Y., Shiratori, H., Mochida, K., Ikawa, Y., Saijoh, Y., Hamada, H., 2001. The transcription factor FoxH1 (FAST) mediates Nodal signaling during anterior-posterior patterning and node formation in the mouse. Genes Dev. 15, 1242–1256.

Yamamoto, M., Mine, N., Mochida, K., Sakai, Y., Saijoh, Y., Meno, C., Hamada, H., 2003. Nodal signaling induces the midline barrier by activating Nodal expression in the lateral plate. Development 130, 1795–1804.

Yan, Y.T., Gritsman, K., Ding, J., Burdine, R.D., Corrales, J.D., Price, S.M., Talbot, W.S., Schier, A.F., Shen, M.M., 1999. Conserved requirement for EGF-CFC genes in vertebrate left–right axis formation. Genes Dev. 13, 2527–2537.

Yang, J.T., Hynes, R.O., 1996. Fibronectin receptor functions in embryonic cells deficient in alpha 5 beta 1 integrin can be replaced by alpha V integrins. Mol. Biol. Cell 7, 1737–1748.

Yang, J.T., Rayburn, H., Hynes, R.O., 1993. Embryonic mesodermal defects in alpha 5 integrin-deficient mice. Development 119, 1093–1105.

Yang, J.T., Rayburn, H., Hynes, R.O., 1995. Cell adhesion events mediated by alpha 4 integrins are essential in placental and cardiac development. Development 121, 549–560.

Yang, J.T., Bader, B.L., Kreidberg, J.A., Ullman-Cullere, M., Trevithick, J.E., Hynes, R.O., 1999. Overlapping and independent functions of fibronectin receptor integrins in early mesodermal development. Dev. Biol. 215, 264–277.

Yelon, D., 2001. Cardiac patterning and morphogenesis in zebrafish. Dev. Dyn. 222, 552–563.

Yoshioka, H., Meno, C., Koshiba, K., Sugihara, M., Itoh, H., Ishimaru, Y., Inoue, T., Ohuchi, H., Semina, E.V., Murray, J.C., et al., 1998. Pitx2, a bicoid-type homeobox gene, is involved in a lefty-signaling pathway in determination of left–right asymmetry. Cell 94, 299–305.

Yost, H.J., 1992. Regulation of vertebrate left–right asymmetries by extracellular matrix. Nature 357, 158–161.

Zovein, A.C., Luque, A., Turlo, K.A., Hofmann, J.J., Yee, K.M., Becker, M.S., Fassler, R., Mellman, I., Lane, T.F., Iruela-Arispe, M.L., 2010. Beta1 integrin establishes endothelial cell polarity and arteriolar lumen formation via a Par3-dependent mechanism. Dev. Cell 18, 39–51.